

# Fluorescence Evidence for Cholesterol Regular Distribution in Phosphatidylcholine and in Sphingomyelin Lipid Bilayers

Parkson Lee-Gau Chong,<sup>1,4</sup> Fang Liu,<sup>1</sup> Mei Mei Wang,<sup>1</sup> Khanh Truong,<sup>1</sup> Istvan P. Sugar,<sup>2</sup> and Rhoderick E. Brown<sup>3</sup>

Received February 12, 1996; accepted October 7, 1996

---

Our previous studies indicated that sterols (including cholesterol and dehydroergosterol) can be regularly distributed into hexagonal superlattices in the plane of liquid-crystalline phosphatidylcholine bilayers. It was suggested that regular and irregular regions coexist in the membrane. In the present study, we report supporting evidence for our sterol regular distribution model. We have examined the fractional concentration dependencies of dehydroergosterol (a naturally occurring cholesterol analogue) fluorescence intensity and lifetime in various phosphatidylcholine and sphingomyelin bilayers. Fluorescence intensity and lifetime dips have been observed at specific sterol mole fractions. At those mole fractions, the acrylamide quenching rate constant of dehydroergosterol fluorescence reaches a local maximum. Those mole fractions match the critical sterol mole fractions at which sterol molecules are expected to be regularly distributed into hexagonal superlattices. The results support the idea that the sterols in the regular region are embedded in the bilayer less deep than those in the irregular regions. We have also examined the fractional cholesterol concentration dependencies of diphenylhexatriene (DPH) fluorescence intensity, lifetime, and polarization in DMPC vesicles. DPH fluorescence intensity and polarization also exhibit distinct dips and peaks, respectively, at critical sterol mole fractions for hexagonal superlattices. However, DPH lifetime changes little with sterol mole fraction. As a comparison, the fluorescence properties of DHE and DPH behave differently in response to the formation of sterol regular distribution. Furthermore, finding evidence for sterol regular distribution in both phosphatidylcholine and sphingomyelin membranes raises the possibility that sterol regular distribution may occur within phospholipid/cholesterol enriched domains of real biological membranes.

---

**KEY WORDS:** Cholesterol; dehydroergosterol; diphenylhexatriene; sterol lateral organization; regular distribution, membranes; phospholipids.

## INTRODUCTION

Cholesterol is one of the major lipid components in mammalian cell membranes. Cholesterol has no reactive functional groups except for the 3 $\beta$ -OH; thus its inter-

action with proteins or lipids in the membrane is most likely to be physical, rather than chemical, in nature. For this reason, previous studies of the interactions of cholesterol with other membrane components were focused on cholesterol lateral organization in the membrane and the effect of cholesterol on membrane dynamics. Dynamic studies indicate that cholesterol causes a condensing effect on its neighboring lipid acyl chains in liquid crystalline bilayers. However, no unequivocal conclusion has been established with regard to cholesterol lateral organization in membranes.

<sup>1</sup> Department of Biochemistry, Temple University School of Medicine, Philadelphia, Pennsylvania 19140.

<sup>2</sup> Departments of Biomathematical Sciences and Physiology & Biophysics, Mount Sinai Medical Center, New York, New York 10029.

<sup>3</sup> Hormel Institute, University of Minnesota, Austin, Minnesota 55912.

<sup>4</sup> To whom correspondence should be addressed.

A number of studies on phospholipid model membranes have suggested the existence of cholesterol-rich domains. For example, Lentz *et al.*<sup>(1)</sup> suggested that cholesterol-rich and cholesterol-poor fluid phases coexist in phospholipid bilayers. Using computer simulations, Snyder and Freire<sup>(2)</sup> found that cholesterol molecules form many random microdomains and that those small domains link into a network at 22 mol% cholesterol. These random domains are, however, different from the aligned cholesterol domains proposed by Rogers *et al.*,<sup>(3)</sup> who suggested that cholesterol molecules in the phospholipid matrix are aligned along a common axis. The alignment would result in macroscopic cholesterol-rich stripe domains where the phospholipids form ribbons between the aligned cholesterol domains. In contrast to domain formation, cholestatrienol, a fluorescent cholesterol analogue, has been reported to be homogeneously dispersed in 1-palmitoyl-2-oleoyl-L- $\alpha$ -phosphatidylcholine (POPC) at sterol/phosphatidylcholine (PC) ratios of less than 0.5.<sup>(4)</sup> Hence, our understanding of cholesterol lateral organization in the plane of membrane is far from clear.

In theory, the lipid molecules in binary mixtures can be either domain segregated, randomly distributed, or regularly distributed.<sup>(5)</sup> This lateral distribution depends on the mixing ratio, temperature, and pressure and on intermolecular energies. In the case of lattice models of membranes, the effect of different intermolecular energies manifests through the energy function  $W(r)$ , defined as  $W(r) = E_{12}(r) - [E_{11}(r) + E_{22}(r)]/2$ , where  $E_{ij}(r)$  refers to the interaction energy between the  $i$ th and the  $j$ th membrane component and  $r$  is the distance between the interacting lipids given in lattice units. At  $W(r) > 0$ , lipid molecules which are similar attract each other more strongly than lipid molecules which are different. Thus, similar molecules tend to form clusters. At  $W(r) = 0$ , all the lipid molecules are distributed randomly in the membrane. At  $W(r) < 0$ , the molecules which are different attract each other more strongly than the molecules which are similar. These are nonideal mixtures possessing a negative deviation from ideality. In this case, the guest molecules are surrounded preferentially by matrix lipids. In 1991, our group pointed out<sup>(6)</sup> that cholesterol tends to be surrounded by the matrix dipalmitoylphosphatidylcholine (DPPC) lipids because calorimetric data for cholesterol in DPPC vesicles showed a negative deviation from ideality ( $W < 0$ ).<sup>(7)</sup> However,  $W < 0$  alone does not provide sufficient evidence for sterol regular distribution. A regular distribution is a lipid lateral organization in the plane of the membrane, where the guest molecules (cholesterol in this case) are maximally sep-

arated into a well-defined regular pattern in the lipid matrix.

The first experimental evidence for sterols being regularly distributed in hexagonal superlattices within liquid crystalline phospholipid bilayers was reported by our group in 1994.<sup>(8)</sup> We found that the fractional concentration dependence of dehydroergosterol ( $\Delta^{5,7,9,(11),22}$ -ergostatriene-3 $\beta$ -ol; DHE) fluorescence in the liquid crystalline state of dimyristoylphosphatidylcholine (DMPC) multilamellar vesicles exhibits many distinct fluorescence intensity drops at specific DHE mole fractions (referred to as DHE intensity dips). Those mole fractions are close to the critical sterol mole fractions predicted by the extended hexagonal superlattice model.<sup>(8-10)</sup> DHE is a naturally occurring fluorescent sterol with its physical and physiological properties resembling ergosterol and cholesterol. Based on the observation of DHE dips and the physical principles underlying lipid regular distribution that we learned from our previous studies on pyrene-labeled phospholipid bilayers,<sup>(10-12)</sup> we have proposed a general model for sterol lateral organization in membranes.<sup>(8)</sup> Our model includes the following essential elements. (i) Sterol molecules tend to be maximally separated and regularly distributed in a hexagonal lipid matrix. (ii) The difference in cross-sectional area between the bulky steroid ring and the matrix phospholipid acyl chain causes an elastic deformation in the hexagonal lipid lattice. This deformation provides the driving force (a repulsive interaction between bulky moieties) for maximal separation of the bulky lipids. (iii) Due to thermal fluctuation, changes in vesicle curvature and the presence of impurities, irregular distributions always coexist with regular distributions. (iv) The ratio of regular distributions to irregular distributions reaches a local maximum at critical sterol mole fractions and a local minimum between two consecutive critical sterol mole fractions.<sup>(12)</sup> (v) The critical sterol mole fractions can be predicted from Eqs. (1) and (2) on the basis of the extended hexagonal superlattice model.<sup>(8-10)</sup> For a given cholesterol molecule, its position in the hexagonal lattice can be described by two integer coordinates ( $n_a, n_b$ ) once the origin and the principal axes are specified (Fig. 1). For cholesterol concentrations less than 30 mol%, the critical cholesterol mole fraction,  $Y$ , at which the cholesterol molecules form regularly distributed hexagonal superlattices can be calculated by Eq. (1).<sup>(8)</sup>

$$Y = 2/(n_a^2 + n_a n_b + n_b^2 + 1) \quad (1)$$

Above 30 mol%, the critical sterol concentrations,  $Y'$ , at which the matrix lipid acyl chains form hexagonal superlattices, can be predicted by Eq. (2)<sup>(8)</sup>

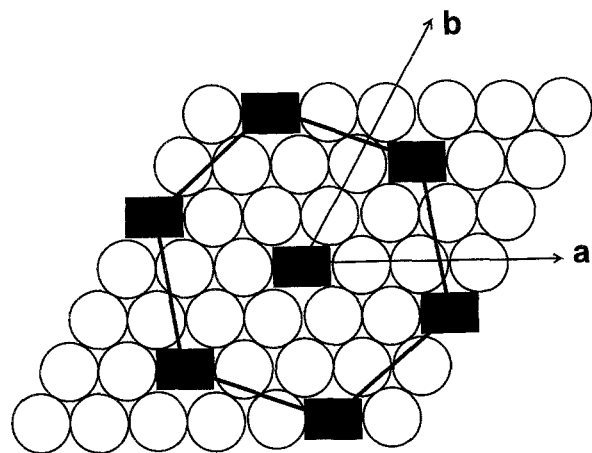


**Fig. 1.** Schematic diagram for the regular distribution pattern of 25 mol% sterol (filled squares) in a diacylphospholipid matrix. The open circles are the acyl chains of diacylphospholipids.

$$Y' = 1 - [2/(m_a^2 + m_a m_b + m_b^2)] \quad (2)$$

where  $m_a$  and  $m_b$  are the projection along the principal axis  $a$  and  $b$ , respectively, for an acyl chain of the matrix phospholipid. (vi) Membrane-free volume is more abundant in irregular regions than in regular regions. Since there are many critical mole fractions over a wide range of sterol concentrations, membrane free volume varies with sterol mole fraction in a periodic manner with a local minimum in membrane free volume at critical sterol mole fractions. (vii) In the regular region, sterol molecules are embedded less deep in the bilayer than those in the irregular region.

In the present study we have provided additional supporting evidence for sterol regular distribution and have tested the validity of our sterol regular distribution model. We have examined the local sterol concentration effect on the steady-state polarization, intensity, and lifetime of diphenylhexatriene (DPH) fluorescence in cholesterol/phosphatidylcholine multilamellar vesicles. In addition, we have used DHE fluorescence lifetime and intensity to demonstrate the existence of sterol regular distribution in DHE/cholesterol/DMPC mixtures. Furthermore, we have used acrylamide quenching of DHE fluorescence to test whether the accessibility of DHE to the water soluble quencher, acrylamide, varies with sterol content in accordance with the principle of lipid regular distribution. Finally, we have extended our studies from phosphatidylcholine bilayers to sphingomyelin bilayers, to illustrate the generality of sterol regular distribution in liquid-crystalline bilayers. A preliminary report of this work has been presented in the 1996 SPIE meeting at San Jose, California.<sup>(33)</sup>

## MATERIALS AND METHODS

Dehydroergosterol (DHE) and cholesterol were obtained from Sigma (St. Louis, MO). Cholesterol was recrystallized from ethanol. The concentration of cholesterol was calculated from weight determinations. DHE was purified by high-performance liquid chromatography with a C-18 reverse-phase column using methanol/acetonitrile (67:33, v/v) as the mobile phase. The concentration of DHE was determined using an extinction coefficient at 326 nm equal to  $10,600 M^{-1} \text{ cm}^{-1}$  (in dioxane). DMPC was purchased from Avanti Polar Lipids (Alabaster, AL) and used as such. Sphingomyelin was produced by reacylating sphingosylphosphocholine using the *N*-hydroxysuccinimide esters of acyl chains enriched in palmitate.<sup>(25)</sup> The phospholipid concentration was determined by the method of Bartlett.<sup>(13)</sup> DPH was purchased from Molecular Probes (Eugene, OR). Acrylamide was recrystallized from ethanol. In this study, the errors of fractional composition resulting from lipid concentration determinations were estimated to be 0.5 mol%.

Appropriate amounts of probes, sterols, and DMPC were first mixed in chloroform. The mixtures were then dried under nitrogen in Eppendorf vials and placed under high vacuum overnight. The dried mixtures were suspended in an aqueous medium. The dispersion was vortexed for 3 min at 40°C for sterols/DMPC mixtures and at 55°C for sterols/sphingomyelin mixtures. These temperatures are above the phase transition temperatures of the matrix lipids (e.g., DMPC and sphingomyelin). The samples were cooled to 4°C for 30 min and then incubated at 40°C for sterols/DMPC mixtures (or at 55°C for sterols/sphingomyelin mixtures) for 30 min. This cooling/heating cycle was repeated two more times. Finally, the samples were stored at room temperature ( $\sim 25^\circ\text{C}$ ) for at least 4 days prior to fluorescence measurements.

Fluorescence intensity measurements were made with an SLM DMX-1000 fluorometer (SLM Instruments, Urbana, IL). For DHE measurements, samples were excited at 324–328 nm. The emission was observed through a monochromator. Steady-state polarization measurements of diphenylhexatriene (DPH) fluorescence were made on an ISS K2 fluorometer (Champaign, IL) using an L-format optical arrangement. Excitation wavelength used was 350 nm, with an excitation bandwidth of 8 nm. Emission was collected through a Schott KV 389 cutoff filter. Blank readings from membrane preparations without probes were subtracted from the sample readings. DPH/DMPC was  $\sim 1/500$ . For intensity and polarization measurements, samples were measured while stirring. Fluorescence lifetimes were determined

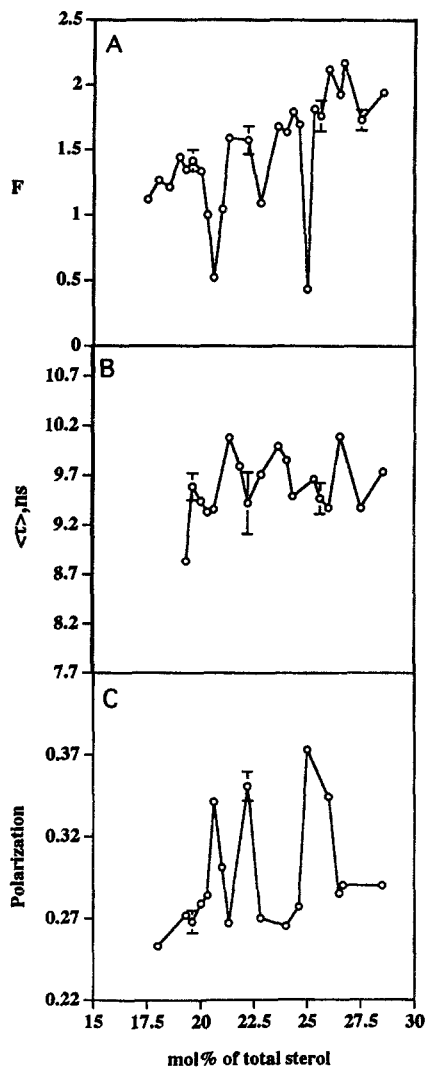


Fig. 2. Effect of cholesterol content on DPH (A) fluorescence intensity,  $F$  (measured at 450 nm), (B) average lifetime,  $\langle\tau\rangle$ , and (C) steady-state polarization in cholesterol/DMPC multilamellar vesicles at 35°C. The error bars indicate the errors from three independently prepared samples. The samples were incubated at room temperature for 1 week prior to the measurement.

using an ISS K2 (Champaign, IL) phase-modulation fluorometer. For DHE lifetime measurements, the light source was a He-Cd laser (Model 4240B, LiConix Inc., Sunnyvale, CA) with excitation at 325 nm. For DPH lifetime measurements, the light source was a xenon arc lamp and the excitation wavelength was 350 nm. For both measurements, the excitation polarizer was set at 35° with respect to the vertical plane, and no emission polarizer was used. Phase and modulation values were determined relative to a *p*-bis[2-(5-phenyloxazoly)]benzene (POPOP) reference solution (in ethanol),

which has a lifetime of 1.35 ns. A Schott KV-389 cutoff filter was used for both DHE and DPH emission intensity decay measurements. For all the fluorescence measurements, the temperature of the sample was controlled by a circulating bath.

## RESULTS

In our previous study,<sup>(8)</sup> a number of DHE intensity dips were observed in the concentration range of 0–55 mol% DHE in DMPC. However, for the purpose of comparison between the theoretical and the observed values, the dips in the intermediate concentration region (e.g., 17–27 mol% sterol) turn out to be more useful because those dips are more separated and can be more easily recognized.<sup>(8)</sup> For this reason, this study was focused on two critical sterol mole fraction regions (i.e., two dips): one centered at 20 mol% sterol and the other at 25 mol%. From our previous study,<sup>(11)</sup> we also knew that lipid regular distribution appears favorably in the liquid-crystalline state of the bilayer. Thus, this study was focused on the membrane properties in the liquid-crystalline state and the experiments were performed at temperatures above the phase transition temperature of the matrix lipid.

It is well established that steady-state fluorescence polarization of DPH in membranes reflects mainly the molecular order of lipid acyl chains. According to our model,<sup>(8)</sup> membrane free volume should reach a local minimum at a critical sterol mole fraction. Thus at the critical sterol concentration, the DPH polarization should be high relative to that at its neighboring noncritical mole fractions. At the 23rd Steenbock Symposium held at the University of Wisconsin—Madison in May 1994, we reported that the steady-state polarization of DPH fluorescence in cholesterol/DMPC mixtures reaches a local maximum at ~20 mol% cholesterol,<sup>(14)</sup> a critical mole fraction for sterol regularly distributed in hexagonal superlattices. We then predicted that this phenomenon should also occur at other critical sterol mole fractions. Figure 2C shows that this is indeed the case. The plot of DPH steady-state fluorescence polarization vs cholesterol mole fraction exhibits a local maximum at 20.6, 22.2, and 25.0 mol%. The 25.0 mol% is one of the critical sterol mole fractions predicted by the hexagonal superlattice model,<sup>(8)</sup> whereas the 22.2 mol% peak is predicted by the centered rectangular superlattice model.<sup>(20)</sup> It should be mentioned that the polarization peak at 25.0 mol% is a representative graph of four sets of experiments, all of which show a local maximum near 25 mol% cholesterol. However, the extent of polariza-

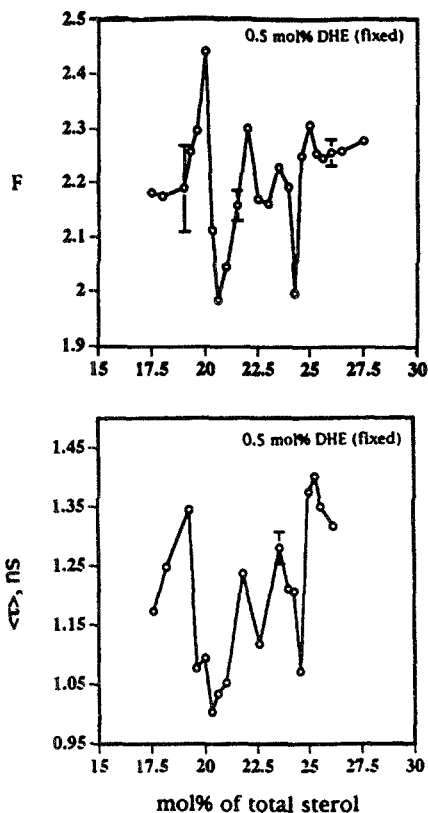


**Fig. 3.** Sterol concentration dependencies of DHE fluorescence intensity and lifetime obtained from DHE/cholesterol/DMPC multilamellar vesicles (with DHE fixed at 0.5 mol%) in 50 mM KCl at 35°C. [Lipid] was  $\sim 300 \mu\text{M}$ .  $F$  is the intensity measured at 378 nm. For intensity measurements, excitation and emission monochromator bandwidths were 2 and 8 nm, respectively. Error bars were determined from three independently prepared samples. Samples were incubated at room temperature for 10 days prior to intensity measurements and for  $>17$  days prior to lifetime measurements.

tion difference between the local maximum and the local minimum varies from experiment to experiment.

Figure 2A shows the sterol concentration dependence of the intensity of DPH fluorescence in DMPC/cholesterol mixtures. Three distinct intensity dips were detected, at 20.6, 22.5, and 25.0 mol%. They match the polarization peaks observed in Fig. 2C. The emission decay of DPH fluorescence in cholesterol/DMPC multilamellar vesicles was determined using modulation frequencies ranging from 15 to 70 MHz. The data are best fit by a two exponential decay law:  $F(t) = \alpha_1 \exp(-t/\tau_1) + \alpha_2 \exp(-t/\tau_2)$ . Figure 2B shows the effect of total sterol on the average lifetime  $\langle\tau\rangle$  of DPH fluorescence.  $\langle\tau\rangle$  was calculated from the equation  $\langle\tau\rangle = f_1\tau_1 + f_2\tau_2$ , where  $f_1$  and  $f_2$  are the fractional intensities. The average lifetime of DPH fluctuates at  $9.6 \pm 0.5$  ns over the concentration range 18–28 mol% cholesterol.

Figure 3 shows the fractional sterol concentration dependencies of DHE fluorescence intensity (top) and average lifetime (bottom) in DHE/cholesterol/DMPC multilamellar vesicles (with DHE fixed at 0.5 mol%) at 35°C. Here the mol% of total sterol equals the mol% of DHE plus the mol% of cholesterol. DHE fluorescence intensity dips are clearly observable at 20.6 and 25.0 mol% of total sterol. These concentrations are close to the theoretical values, 20 and 25 mol%, predicted for sterol regular distribution in hexagonal superlattices. In Fig. 3 the additional (small) DHE dip at 22.2 mol% is predicted by the centered rectangular superlattice model.<sup>(20)</sup> Note that in Fig. 2 DPH intensity and DPH polarization also exhibit a peculiar behavior near 22.2 mol%.

The emission decay of DHE fluorescence in DHE/cholesterol/DMPC multilamellar vesicles was determined using modulation frequencies ranging from 30 to 200 MHz. The data are best fit by a two-exponential decay law:  $F(t) = \alpha_1 \exp(-t/\tau_1) + \alpha_2 \exp(-t/\tau_2)$ . Figure 3 (bottom) shows the effect of total sterol on the average lifetime  $\langle\tau\rangle$  of DHE fluorescence.  $\langle\tau\rangle$  was calculated from the equation  $\langle\tau\rangle = f_1\tau_1 + f_2\tau_2$ . DHE fluorescence lifetime dips are readily observable at 20.3 and 24.6 mol% total sterol, which are also near the critical sterol mole fractions (i.e., 20 and 25 mol% of total sterol) predicted for sterols regularly distributed into hexagonal superlattices. Again, a small lifetime dip observed at 22.5 mol% can be attributed to the critical sterol mole fractions predicted for centered rectangular superlattices.<sup>(20)</sup>

Figure 4 shows the typical Stern–Volmer plots of acrylamide quenching of DHE fluorescence intensity in DHE/DMPC mixtures at 35°C. The slope of the plot gives the Stern–Volmer constant  $K_{SV}$ , which exhibits a local maximum at 20.6 and 24.4 mol% DHE (Fig. 5). These concentrations are close to the predicted critical mole fractions (i.e., 20 and 25 mol%) for sterol regular distribution into hexagonal superlattices. Although these two observed values deviate slightly from the theoretical values, they nevertheless match with the DHE fluorescence intensity dips (Fig. 5) measured from the same samples. The slight deviation can be attributed to experimental errors. Using the average lifetime  $\tau_0$  (Fig. 5) determined in the absence of acrylamide and assuming a dynamic quenching mechanism, the bimolecular quenching rate constant  $k_q$  can be calculated using the equation  $F_0/F = 1 + k_q\tau_0[\text{acrylamide}] = 1 + K_{SV}[\text{acrylamide}]$ . The calculated  $k_q$  values (Fig. 5) exhibit a local maximum at 20.6 and 24.4 mol% DHE. It should be mentioned that, in Fig. 5, we do not have enough data points with small concentration intervals between 21 and 24 mol% to exhibit the 22.2 mol% dip

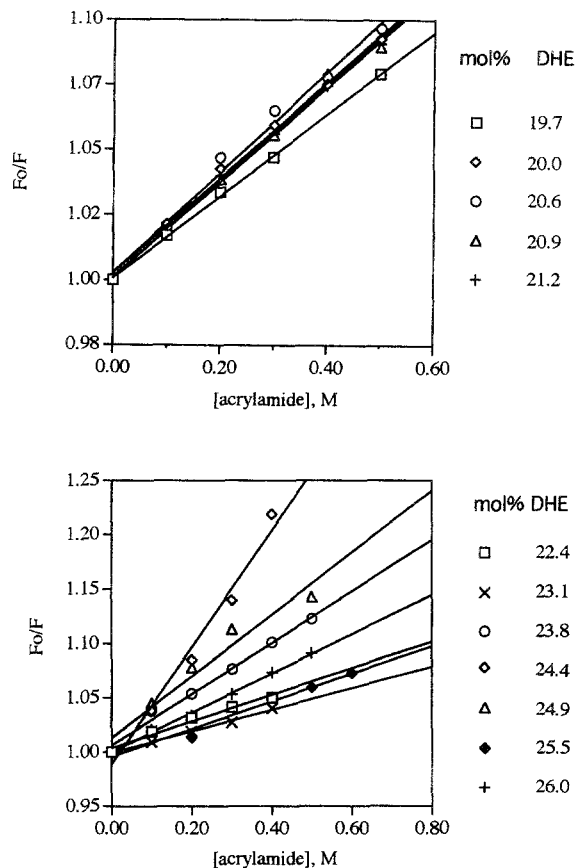
or peak, as shown in Figs. 2 and 3. This is because the quenching experiment requires a much longer time and too many samples would make it difficult to assure identical thermal history for all the samples.

Figure 6 shows the plot of DHE fluorescence intensity as a function of DHE mole fraction in DHE/sphingomyelin multilamellar vesicles at 48°C. Two distinct intensity dips are detected, at 20.6 and 24.4 mol% DHE. The same dip positions were observed from two independent sample preparations (Experiments 1 and 2). These two concentrations are close to the critical sterol mole fractions (20 and 25 mol%, respectively) predicted for sterol regular distribution into hexagonal superlattices, suggesting that sterol regular distribution occurs not only in DMPC but also in sphingomyelin.

## DISCUSSION

Cholesterol is known to cause a condensing effect on its neighboring lipid acyl chain. We have previously used the concept of cholesterol condensation effect and the data of DHE dips to propose a new model for cholesterol lateral distribution in membranes (Fig. 2 in Ref. 8). According to our model, when the cholesterol content is over 30 mol% at 35°C, virtually all DMPC acyl chains in the regularly distributed areas are nearest neighbors of cholesterol (e.g., Fig. 2C in Ref. 8). At such high sterol concentrations, most membrane lipid acyl chains are ordered by cholesterol, if the membrane is dominated by regular areas. Thus, regular distribution is not incompatible with the presence of the liquid-ordered phase [26 and references cited therein]. Similarly, when the cholesterol content is low (e.g., <10 mol%), the amount of lipid acyl chains being nearest neighbors of cholesterol is small, even if all the cholesterol molecules in the membrane are regularly distributed (e.g., maximally separated). Thus, at low sterol concentrations, lipid acyl chains are mainly in the liquid-disordered state at 35°C in cholesterol/DMPC mixtures. In the intermediate concentrations 10–30 mol%, liquid-ordered and liquid-disordered phases coexist.

The concept of sterol regular distribution not only is compatible with the concept of liquid-ordered and liquid-disordered phases, but also points out that the phase diagram of DMPC/cholesterol may be more complicated than currently thought [26,31 and references cited therein]. Our measurements have been performed in a temperature and concentration range where two liquid crystalline phases,  $\alpha$  and  $\beta$  (i.e., liquid-disordered and liquid-ordered phases), coexist.<sup>(26)</sup> We selected this region because within the mixed-phase region (at 35°C



**Fig. 4.** Effect of membrane DHE content on the relationship between  $F^0/F$  and acrylamide concentration for DHE in DMPC multilamellar vesicles at 35°C.  $F^0$  is the intensity in the absence of acrylamide.  $F$  was determined as an integrated fluorescence intensity from 340 to 460 nm. The aqueous medium was 0.1 M Tris, pH 7.1. The concentration of lipids used for the measurements was  $\sim 51 \mu\text{M}$ . The intensities were corrected for background signals and for volume changes.

from 10 to 30 mol% sterol), the dips are more pronounced and well separated,<sup>(8)</sup> although the dips in the pure  $\alpha$ - and  $\beta$ -phase regions also were detected.<sup>(8)</sup> Normally, within a mixed phase region every physical parameter of the system changes continuously when the concentration is increased at a fixed temperature. Singularities can be expected only at the phase boundaries. Our fluorescence measurements are sensitive enough to detect several singularities (dips)<sup>(8)</sup> within and without the  $\alpha + \beta$  mixed-phase region at certain critical concentrations. In our view, every critical concentration marks the presence of a phase boundary.<sup>(12)</sup>

The steady-state polarization of DPH fluorescence reflects mainly the molecular order of lipid acyl chains. If the membrane free volume reaches a local minimum at a critical sterol mole fraction,<sup>(8,11)</sup> then DPH polarization should be higher at critical cholesterol mole frac-

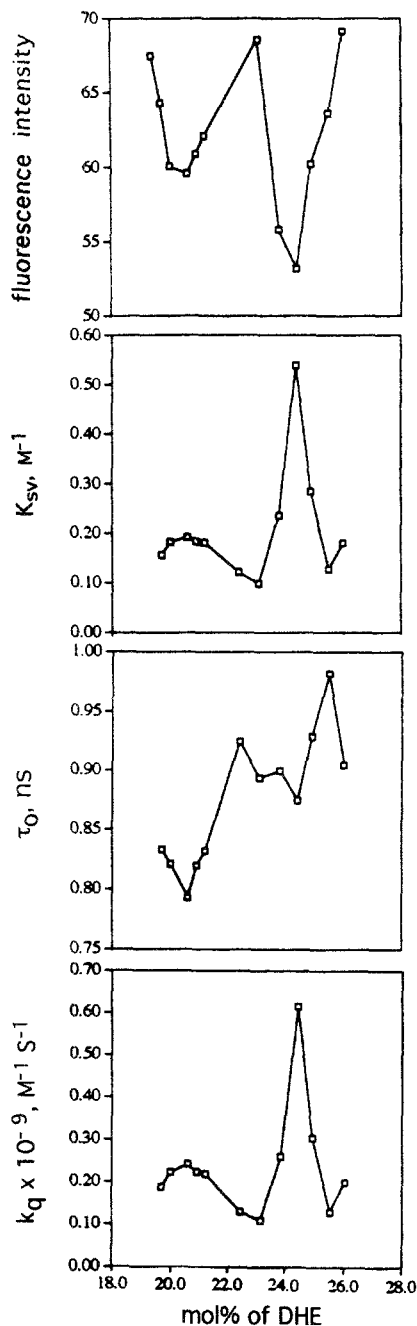


**Fig. 5.** Concentration dependencies of DHE fluorescence intensity in the absence of acrylamide, the Stern-Volmer constant  $K_{SV}$ , the average lifetime of DHE fluorescence in the absence of acrylamide  $\tau_0$ , and the quenching rate constant  $k_q$  in the 20 and 25 mol% dip regions for DHE/DMPC mixtures at 35°C. Samples in these two regions (19.7–21.2 mol and 22.4–26.0 mol%) were measured on different dates, thus experiencing different thermal histories. The data on  $K_{SV}$  were derived from those shown in Fig. 4.

tions than at their neighboring noncritical mole fractions if the lifetime changes little with cholesterol mole frac-

tion. As shown in Fig. 2 and Ref. 14, the steady-state DPH fluorescence polarization indeed exhibits a local maximum near 20 and 25 mol% cholesterol, and DPH lifetime varies little with sterol mole fractions; 20 and 25 mol% are two of the critical mole fractions predicted for cholesterol regularly distributed in diacylphosphatidylcholine bilayers.<sup>(8,20)</sup> As previously shown by many investigators (e.g., Refs. 23 and 24), there is an increasing trend in the steady-state DPH fluorescence polarization as the cholesterol content in the membrane increases from 0 to 50 mol%. This is a global effect of lipid acyl chain ordering by cholesterol. What we are showing here<sup>(14)</sup> (Fig. 2C) is a local concentration effect. This local cholesterol concentration effect has been largely ignored in previous studies of membrane properties. In view of the fact that under physiological conditions, the cholesterol content in many cell membranes fluctuates only a few percent,<sup>(15,16)</sup> it is of importance to conduct a full investigation on the local cholesterol concentration effect on membranes. The local cholesterol concentration effect on membranes can be revealed only if small concentration increments (1 mol% or less) are employed.

Figure 2B shows that the average lifetime of DPH changes little with sterol mole fraction, fluctuating at  $9.6 \pm 0.5$  ns over the concentration range 18–28 mol% cholesterol. The small lifetime dips near 20 and 25 mol% sterol are <6% (Fig. 2B); in contrast, deep and sharp intensity dips are observed at 25.0 mol% (~82% change in intensity) and 20.6 mol% (~66% change in intensity) (Fig. 2A). In comparison, Fig. 3 shows a DHE intensity dip at 20.6 mol% sterol with an intensity change of 18% and a DHE lifetime dip at 20.6 mol% with a lifetime change of 26%. Similarly, at 24.8 mol% sterol, the intensity dip shows an intensity change of 14%, whereas the lifetime dip shows a change of 21% (Fig. 3). Intensity measurements and lifetime measurements were done on different dates. The depth of the dip (or the peak height) may vary (e.g., ~20%) with samples' thermal history.<sup>(8)</sup> After considering this factor and the experimental errors, we can say that in the case of DHE, the magnitudes of the depth for the intensity and lifetime dips are similar, but in the case of DPH, they are not. Clearly, the fluorescence properties of DHE and DPH behave differently in response to the formation of sterol regular distribution.

DHE serves as both a lipid component in the membrane and a fluorescent probe. We previously proposed<sup>(8)</sup> that DHE is embedded less deep in the bilayer in the regular region, compared to the irregular region. Since the ratio of regular areas to irregular areas reaches a local maximum at critical sterol mole fractions<sup>(12)</sup> and since

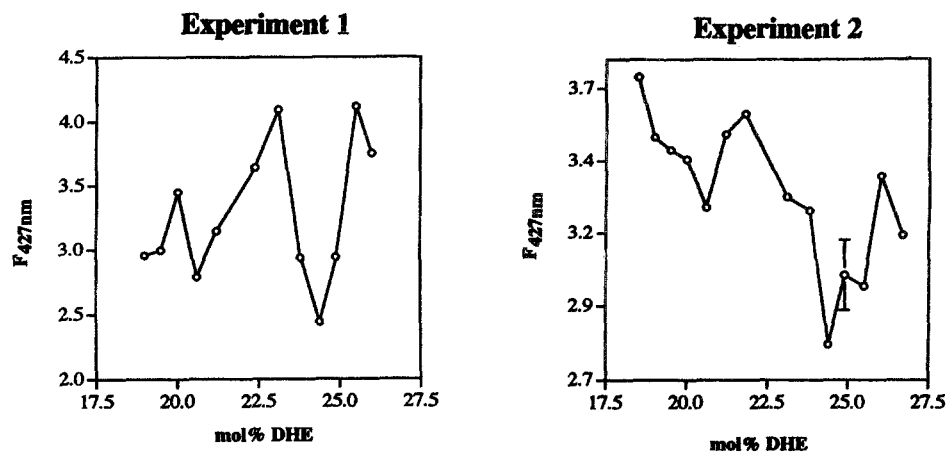


Fig. 6. Concentration dependence of DHE fluorescence intensity in sphingomyelin multilamellar vesicles. F<sub>427</sub> is the fluorescence intensity measured at 427 nm; emission slit width = 8 nm; excitation wavelength = 328 nm. The acyl composition of the sphingomyelin was 94% (16:0), 4.8% (18:0), 0.9% (14:0), and 0.4% (17:0). Temperature = 48°C, which is above the  $T_m$  of 16:0-sphingomyelin.

the fluorescence of DHE has been previously shown to be dependent on the dielectric constant of the medium,<sup>(17)</sup> it is reasonable to observe that both the intensity and the lifetime of DHE fluorescence drop by a similar amount at critical sterol mole fractions (Fig. 3).

In contrast, DPH is not a sterol; it is a free probe. The intensity of DPH fluorescence depends not only on the dielectric constant (reviewed in Refs. 27 and 28) but also on the partitioning of DPH between the aqueous phase and the membrane and may also depend on the partitioning between various microdomains in the membrane (e.g., the liquid ordered and liquid disordered phases). At critical sterol mole fractions, membrane free volume reaches a local minimum.<sup>(8,11)</sup> As a result, the partitioning of DPH in membranes may reach a local minimum, as solute partitioning is known to depend on the membrane surface density<sup>(29)</sup>. Since the quantum yield of DPH in membrane is ~1000 times higher than that in water, even a small decrease in partitioning would bring about a significant decrease in fluorescence intensity. This explains the observation of DPH intensity dips (Fig. 2A). DPH is known to be mainly embedded in the hydrocarbon core of lipid bilayer, in contrast to the location at the interfacial region for the chromophore of DHE. Also, it is likely that DPH prefers to insert into the irregular regions, rather than the regular regions, because the regular region requires a more stringent lattice arrangement. In the irregular region, there is no reason for DPH to undergo dramatic changes in its vertical position when the sterol mole fraction changes; hence, the dielectric constant of the medium near DPH changes little with sterol mole fraction. This explains the inability to observe similar DPH lifetime dips (Fig. 2B) at critical

mole fractions where deep DPH intensity dips are readily observable (Fig. 2A). (Note that DPH lifetime also depends on the dielectric constant of the medium.<sup>(34,35)</sup>) Furthermore, because the overall membrane free volume reaches a local minimum, the steady-state polarization of DPH fluorescence increases at critical sterol mole fractions such as 20 and 25 mol%. Although DPH data support our concept of sterol regular distribution, the concerns with the distribution of DPH make it more difficult to interpret the DPH signal. This highlights the importance of using a sterol probe, such as dehydroergosterol, to study sterol lateral organization.

In our previous study,<sup>(8)</sup> we postulated that, in the regular region, sterol molecules may be embedded somewhat less deep into the bilayer because the regular region contains less membrane free volume. As a result, sterol molecules in the regular region experience a higher dielectric constant than sterol molecules in the irregular region. Since DHE fluorescence is known to decrease with increasing dielectric constant of the medium,<sup>(17)</sup> the fluorescence intensity of dehydroergosterol drops at critical mole fractions where the size of the regular region reaches a local maximum.<sup>(12)</sup>

Our present quenching results fully support the above explanation. The data of the quenching rate constant  $k_q$  (Fig. 5) clearly showed that DHE molecules become more accessible to the water-soluble quencher, acrylamide, at the sterol mole fractions where the DHE fluorescence intensity exhibits a local minimum (a dip) (Fig. 5), whereas the intensity dip positions match with the theoretical values predicted for sterol regular distribution into hexagonal superlattices. Our lifetime data also support the above explanation because the DHE flu-

orescence lifetime displays a local minimum at the sterol mole fractions where the fluorescence intensity exhibits a local minimum (Figs. 3 and 5). This is expected because, like DHE fluorescence intensity, DHE fluorescence lifetime should also decrease with increasing dielectric constant of the surrounding medium.

Our original finding of evidence for sterol regular distribution was based on fluorescence intensity measurements.<sup>(8)</sup> Fluorescence intensity depends on sample concentrations; therefore, it can be argued that the observed intensity dips may result from errors in intensity measurements due to vesicle precipitation and/or the loss of materials during sample transfer between the cuvette and sample vials. However, in this study, we used the concentration-independent parameters, such as lifetime, quenching rate constant, and polarization, to show the occurrence of local minima or maxima in those parameters at the same sterol mole fractions as revealed by the intensity measurements. This argues strongly that our original finding of DHE intensity dips<sup>(8)</sup> is not an artifact of fluorescence measurements.

Our model for sterol lateral organization agrees with the well-known cholesterol condensing effect on lipid acyl chains and is not incompatible with the models of aligned sterol domains<sup>(3)</sup> or homogeneous dispersions.<sup>(4)</sup> In our model, both regular and irregular regions coexist. Sterols are aligned (Figs. 2A–C in Ref. 8) or homogeneously distributed (Figs. 2A and B in Ref. 8) in the regular region. Our model is also consistent with the direct volume measurement made by Melchior *et al.*,<sup>(18)</sup> who showed several local minima and maxima in the plots of partial specific volume *vs* mole fraction of cholesterol in the liquid–crystalline state of DPPC. Moreover, our original findings of evidence for sterol regular distribution have now been supported by spectroscopic data obtained from other groups.<sup>(19,20,30)</sup> Notably, Virtanen *et al.*<sup>(20)</sup> reported not only hexagonal superlattices but also centered rectangular superlattices for cholesterol lateral distribution in DMPC bilayers. After our earlier theoretical<sup>(6,11)</sup> and experimental evidence<sup>(8,14)</sup> regarding sterol regular distribution, Tang *et al.*<sup>(30)</sup> also reported evidence for cholesterol regular distribution.

Sphingomyelin is one of the simplest of polar sphingolipids, which play an important role in certain virus and bacterial toxin binding events at the cell surface, in mediating various signal transduction events, in modulating the behavior of various growth factor receptors [e.g., epidermal growth factor (EGF), nerve growth factor (NGF)], and in forming detergent-insoluble membrane regions involved in glycosylphosphatidylinositol-protein sorting within cells. Our data obtained so far

indicate that DHE dips near 20 and 25 mol%, two critical sterol mole fractions, are clearly observable in phosphatidylcholine and sphingomyelin bilayers, suggesting that sterol regular distribution may have profound functional implications in real biological membranes. In fact, the sphingomyelin used here is very similar to that found in naturally occurring egg yolk with respect to acyl composition [32 and references cited therein].

That the variation in cholesterol concentration by only 1–3 mol% in the vicinity of a critical cholesterol mole fraction causes a significant change in membrane properties would imply that variations in lipid regular distribution by small changes in cholesterol content in the vicinity of a critical cholesterol concentration may serve as a bioswitch which can turn up or down a membrane activity. This would be a new type of regulation in membrane activities and may provide a molecular explanation as to why an optimal cholesterol content is required in cell membranes. This bioswitch effect may also explain why a small change (6 mol%) in cholesterol content of the erythrocyte membrane affects significantly the activity of adenylate cyclase and the activities of phosphoinositide kinases (by ~50%).<sup>(21,22)</sup> (Note that, simply based on the old concept of the global cholesterol condensing effect, one would not think that a 6 mol% change in cholesterol content could significantly alter membrane fluidity.) The above-mentioned enzymes are important in membrane signal transduction; hence, it is conceivable that the bioswitch based on lipid regular distribution may even play a more general regulatory role in membranes.

## ACKNOWLEDGMENTS

This work was supported in part by the American Heart Association (Grant 95010730 to P.L.-G.C.), the Temple University Research Incentive Fund (to P.L.-G.C.), the Federal Work Study program (to K.T.), and NIGMS Grant RO1-45928 (to R.E.B.) for sphingomyelin production. We thank Mr. Anthony A. Golsorkhi for preliminary studies on DPH polarization.

## REFERENCES

1. B. R. Lentz, D. A. Barrow, and M. Hoehli (1980) *Biochemistry* **19**, 1943–1954.
2. B. Snyder and E. Freire (1980) *Proc. Natl. Acad. Sci. USA* **77**, 4055–4059.
3. J. Rogers, A. G. Lee, and D. D. Wilton (1979) *Biochim. Biophys. Acta* **552**, 23–37.
4. P. A. Hyslop, B. Morel, and R. D. Sauerheber (1990) *Biochemistry* **29**, 1025–1038.

5. P. H. Von Dreele (1978) *Biochemistry* **17**, 3939–3943.
6. I. P. Sugar, J. Zeng, and P. L.-G. Chong (1991) *J. Phys. Chem.* **95**, 7524–7534.
7. S. Mabrey, P. L. Mateo, and J. M. Sturtevant (1978) *Biochemistry* **17**, 2464–2468.
8. P. L.-G. Chong (1994) *Proc. Natl. Acad. Sci. USA* **91**, 10069–10073.
9. J. A. Virtanen, P. Somerharju, and P. K. J. Kinnunen (1988) *J. Mol. Electr.* **4**, 233–236.
10. D. Tang and P. L.-G. Chong (1992) *Biophys. J.* **63**, 903–910.
11. P. L.-G. Chong, D. Tang, and I. P. Sugar (1994) *Biophys. J.* **66**, 2029–2038.
12. I. P. Sugar, D. Tang, and P. L.-G. Chong (1994) *J. Phys. Chem.* **98**, 7201–7210.
13. G. R. Bartlett (1959) *J. Biol. Chem.* **234**, 466–468.
14. P. L.-G. Chong (1996) in J. L. Markley, D. B. Northrop, and C. A. Royer (Eds.), *High Pressure Effects in Molecular Biophysics and Enzymology*, Proceedings of the 1994 Steenbock Symposium, Oxford University Press, New York, pp. 298–313.
15. E. Alvarez, V. Ruiz-Gutierrez, C. S. Maria, and A. Machado (1993) *Mech. Age. Dev.* **71**, 1–12.
16. E. Quintao, S. M. Grundy, and E. H. Ahrens (1971) *J. Lipid Res.* **12**, 233–247.
17. F. Schroeder, Y. Barenholz, E. Gratton, and T. E. Thompson (1987) *Biochemistry* **26**, 2441–2448.
18. D. L. Melchior, F. J. Scavitto, and J. M. Steim (1980) *Biochemistry* **19**, 4828–4834.
19. T. Parasassi, A. M. Giusti, M. Raimondi, and E. Gratton (1995) *Biophys. J.* **68**, 1895–1902.
20. J. Virtanen, M. Ruonala, M. Vauhkonen, and P. Somerharju (1995) *Biochemistry* **34**, 11568–11581.
21. G. Puchwein, T. Pfeffer, and E. J. M. Helmreich (1974) *J. Biol. Chem.* **249**, 3232–3240.
22. H. M'Zali, and F. Giraud (1986) *Biochem. J.* **234**, 13–20.
23. P. L.-G. Chong and A. R. Cossins (1984) *Biochim. Biophys. Acta* **772**, 197–201.
24. A. Chabanel, M. Flamm, K. L. P. Sung, M. M. Lee, D. Schachter, and S. Chien (1983) *Biophys. J.* **44**, 171–176.
25. J. M. Smaby, V. S. Kulkarni, M. Momen, and R. E. Brown (1996) *Biophys. J.* **70**, 868–877.
26. C. R. Matteo, A. U. Acuna, and J.-C. Bronchon (1995) *Biophys. J.* **68**, 978–987.
27. D. Topytygin and L. Brand (1995) *J. Fluoresc.* **5**, 39–50.
28. E. Gratton and T. Parasassi (1995) *J. Fluoresc.* **5**, 51–57.
29. L. R. De Young and K. A. Dill (1990) *J. Phys. Chem.* **94**, 801–809.
30. D. Tang, B. W. van der Meer, and S.-Y. S. Chen (1995) *Biophys. J.* **68**, 1944–1951.
31. T. P. W. McMullen and R. N. McElhane (1995) *Biochim. Biophys. Acta* **1234**, 90–98.
32. J. M. Smaby, M. Momen, V. S. Kulkarni, and R. E. Brown (1996) *Biochemistry* **35**, 5696–5704.
33. P. L.-G. Chong, M. M. Wang, F. Liu, K. Truong, A. Golsorkhi, I. P. Sugar, and R. E. Brown (1996) *Proc. Fluoresc. Detect. IV, SPIE* **2705**, 143–154.
34. M. Straume and B. J. Litman (1987) *Biochemistry* **26**, 5121–5126.
35. C. Ho and D. Stubbs (1992) *Biophys. J.* **63**, 897–902.